Aerosol and Air Quality Research, 17: 1909–1916, 2017

ISSN: 1680-8584 print / 2071-1409 online
doi: 10.4209/aaqr.2016.07.0313

Technical Note

Deciphering Effects of Surface Charge on Particle Removal by TiO_2 Polyacrylonitrile Nanofibers

Qian Zhang[1], Fang Liu[2], Tasi-Yu Yang[3], Xv Lv Si[1*], Gong Ren Hu[1], Chang-Tang Chang[3]**

1 College of Chemical Engineering, HuaQiao University, Xiamen 361021, China
[2] College of Environment and Ecology, Xiamen University, Xiamen 361021, China
[3] Department of Environmental Engineering, National Ilan University, Yilan City, Yilan 26047, Taiwan

ABSTRACT

Over the recent years, the continued increase in the number of particles in air has become a public concern. This problem can be addressed by using nanofibers to filter fine particles. However, nanofibers possess complex characteristics. As such, the effects of surface charge require further studies. In this study, the surface voltages of nanofibers were analyzed with an electrometer after these fibers were charged through corona discharge to investigate the mechanism of filtration. Results indicated that the surface voltage of 2.0% TiO_2 polyacrylonitrile fibers (TPFs) can reach up to 0.97 kV and then decrease to 0.60 kV after 96 h. Particles were optimally removed by charged polyacrylonitrile fibers (PFs) and TPFs. Particle penetration decreased by 71% of TPF and 36% of PF. Scanning Electron Microscopy and Nitrogen adsorption/desorption isotherms revealed that increasing the surface area and roughness of these materials are more favorable for charge maintenance to promote particle removal. Our research could provide an in-depth understanding of the effects of surface charge on particle removal and show how systems can be optimized for further applications.

Keywords: Electrospinning; Particle filtration; TiO_2 polyacrylonitrile fibers; Surface charge.

INTRODUCTION

As main air pollutants, particles have become a major public health concern since the emergence of air pollution in developing countries (Especially China) (Lu *et al.*, 2016; Wang *et al.*, 2016; Wen *et al.*, 2016l Zhao *et al.*, 2016). Particle pollutants are closely related to humans because these particles are produced through anthropogenic processes, such as combustion or vehicle emissions. These suspended particle emissions also pose a health risk to humans. For instance, particles larger than 2.5 μm can accumulate in the respiratory tract or lungs (Janssens *et al.*, 2003; Li *et al.*, 2013). Likewise, particles smaller than 2.5 μm may build up in the lungs and adversely affect lung functions; consequently, some diseases may develop (Janssens *et al.*, 2003; Li *et al.*, 2013; Zhu *et al.*, 2016). Cai *et al.* (2015) further reported a linear relationship between cumulative $PM_{2.5}$ concentration and outpatient respiratory diseases. Hence, economic development and its effect on the environment should be balanced, and the influence of these developments on human health should be considered.

Traditional methods, including electrostatic collection (Wettervik *et al.*, 2015), cyclone (Wang *et al.*, 2010), wet washing (Vega *et al.*, 2014), and filtration (Tanabe *et al.*, 2011; Chang *et al.*, 2016), have been applied to reduce particulate pollutant emission and address particle pollution. Among these methods, filtration is the most preferred particle removal approach because of its low cost and small land requirement (Ratnesar-shumate *et al.*, 2008). Nanofibers prepared through electrostatic spinning are potential materials for filtration because these nano-sized fibers can efficiently filter fine air particles. Polymeric nanofibers containing metal oxide nanoparticles have also been widely considered because they possess a large surface area, small pore size, and high porosity (Park *et al.*, 2007). Polymeric nanofibers can strongly influence electrostatic interactions between dust particles and nanofibers (Cho *et al.*, 2013). Polymeric fibers are widely used in various fields (Table 1) (Qiu and Yu, 2008; Doh *et al.*, 2008; Kim *et al.*, 2009; Azad *et al.*, 2010; Francis *et al.*, 2011; Zhang *et al.*, 2011; Li *et al.*, 2012; Nirmala *et al.*, 2012; Batool *et al.*, 2013; Choi *et al.*, 2013; Wang *et al.*, 2015; Zhang *et al.*, 2016). Ratnesar-Shumate *et al.* (2008) found that polymers as poor conductors maintain rather than release the charge generated through

* Corresponding author.
E-mail address: xls895623@126.com
** Corresponding author.
Tel.: 886-3-9357400, fax: 886-3-9359674
E-mail address: ctchang@niu.edu.tw

Table 1. Summary of nanofibers preparation and application.

No.	Material	Method	Polymer	Application	Ref.
1	TiO_2 fiber	Electrostatic spinning	PVP	---	(Qiu and Yu, 2008)
2	TiO_2 fiber	Electrostatic spinning	PVA	Dyes degradation	(Doh *et al.*, 2008)
3	Pt-TiO_2 fiber	Electrostatic spinning	PEO	CO transformation	(Kim *et al.*, 2009)
4	Fe-TiO_2 fiber	Electrostatic spinning	PVP	Sterilization	(Azad *et al.*, 2010)
	Fe-TiO_2 fiber				
5	TiO_2 fiber	Electrostatic spinning	PVP	C_2H_4 degradation	(Li *et al.*, 2012)
6	Hollow TiO_2 fiber	Electrostatic spinning	PVP	CO sensors	(Batool *et al.*, 2013)
7	TiO_2 fiber	Electrostatic spinning	PMMA	Degradation of methylene blue	(Choi *et al.*, 2013)
8	Sn-TiO_2 fiber	Electrostatic spinning	PVP	Methylene blue and methyl orange degradation	(Nirmala *et al.*, 2012)
9	Bi_2WO_6-TiO_2 fiber	Electrostatic spinning	PVP	Degradation of methylene blue	(Zhang *et al.*, 2011)
10	TiO_2 fiber	Electrostatic spinning	PVP	Dye-sensitised solar cells	(Francis *et al.*, 2011)
11	3D nanofibre-nets	Electrostatic spinning	N6–PAN NNB	Particle filtration (Efficiency > 99.99%)	(Wang *et al.*, 2015)
12	PA-6/PMIA NFN	Electrostatic spinning	PA-6	Particle filtration (Efficiency > 99.99%)	(Zhang *et al.*, 2016)
13	PFs/TPFs	Electrostatic spinning	DMAC	Particle filtration (Efficiency > 99.99%)	This Research

electric field stretching on the surface.

The mechanism of particle removal is complex because of multiple factors that work simultaneously. Although some mechanisms, such as interception, inertial impaction, and sieving, involved in filtration with nanofibers have been elucidated, the function of electrostatic attraction requires further studies. The ability of nanofibers to maintain charges is key to understanding charge stability. The charge stabilities of some materials, such as polyacrylonitrile (Schreuder-Gibson, *et al.*, 2005), polystyrene (Schreuder-Gibson, *et al.*, 2005), polycarbonate (Collins *et al.*, 2012), and polyacrylonitrile (Collins *et al.*, 2012), have been analyzed, but the relationship between surface charge and particle deposition has been seldom discussed. Hence, this study investigated the relationship between surface charge and particle removal efficiency by TiO_2 polyacrylonitrile nanofibers. The individual and interactive effects of operating parameters, including TiO_2 loading, face velocity, and surface voltage, on the treatment efficiency of particles were also explored. Nanofiber characteristics were analyzed through Scanning Electron Microscopy and Nitrogen adsorption/desorption isotherms, and electrometry.

EXPERIMENTAL METHODS

Preparation of Polyacrylonitrile Fibers (PFs) and TiO_2 PFs (TPFs)

PFs and TPFs were synthesized through electrospinning by using the following raw materials: polyacrylonitrile powder (Aldrich), dimethylacetamide (DMAC, Sinopharm), and TiO_2 (Digussa, P25). In typical PF preparation, 1 g of polyacrylonitrile powder was first mixed with 20 mL of DMAC solution at 60°C. The solution was then magnetically stirred for 6 h and ultrasonically vibrated for 1 h to obtain a precursor solution. Then, the PFs were prepared through electrospinning with a 10 ml syringe (0.52mm in diameter) and stainless steel needles. The applied voltage between the tips and the collector ranged from 13 kV to 16 kV, and the distance was 15 cm. The feed rate was 1.0 mL h^{-1}, and a syringe pump with a rotating metal drum (diameter, 8 cm; rotation speed, 100 rpm; rotation rate, 20–30 cm s^{-1}) wrapped with spunbondnylon was used to collect the PFs.

In TPF preparation, 1 g of polyacrylonitrile powder and a certain amount of TiO_2 were initially mixed with 20 ml of DMAC solution as a precursor solution at 60°C. Then, the same process as PF preparation was carried out. A schematic of the preparation method is shown in Fig. 1(a). The prepared fibers, due to slightly charged after electrospinning, were named as "Initial charged fibers" to distinguish from the "corona-charged fibers" prepared subsequently.

Corona Charging of PFs and TPFs

In PF and TPF charging, the air was fed into the syringe with stainless steel needles instead of the precursor solution. The syringe was connected to a 16 kV voltage source at a distance of 15 cm, while the PFs and TPFs were used as grounded collectors. The feed rate was 1.0 mL h^{-1}, and a syringe pump with a rotating metal drum (diameter, 8 cm; rotation speed, 100 rpm; rotation rate, 20–30 cm s^{-1}) was

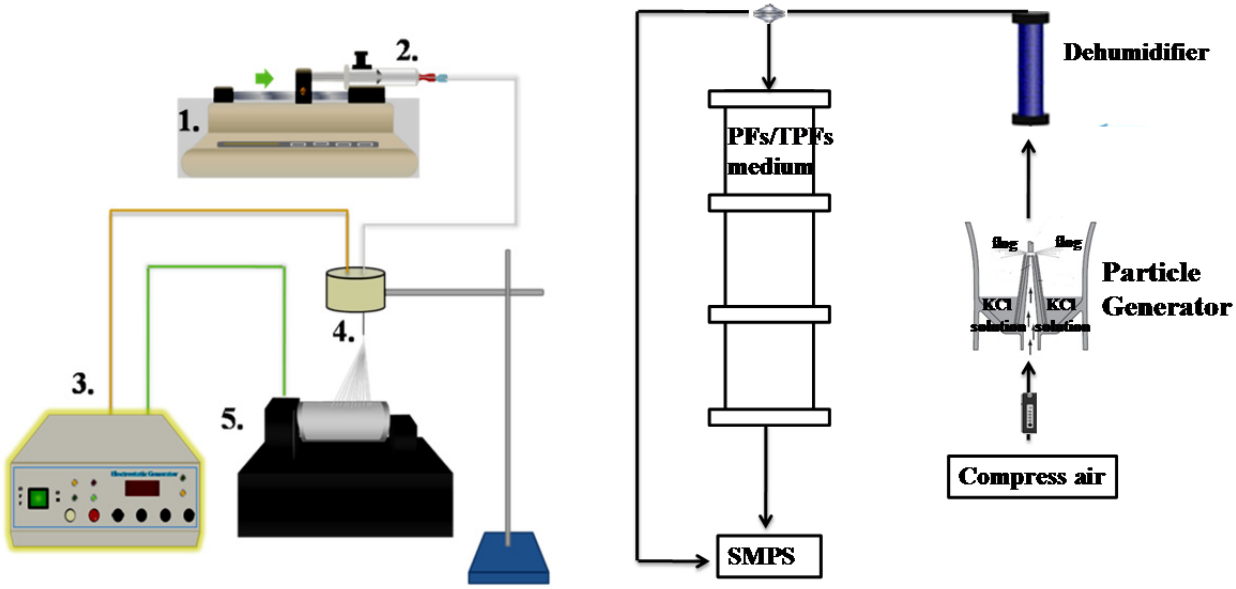

(a) (b)

Fig. 1. (a) The experimental flowchart of TPFs preparation (1.The quantitative syringe, 2.cylinder, 3. high voltage supply, 4. needles, 5. Rotate the collector) (b) Filtration progress.

wrapped for 1 h. During charging, the temperature and humidity of the reaction were controlled at 25°C and 45%.

Progress of Filtration

A filtration was carried out in a columnar reactor. The charged PFs/TPFs under different dosages or the initial charged PFs/TPFs were fixed as filter medium in a stainless steel clip. The size of the column used in this research was 60 cm × 2.5 cm × 2.5 cm. The experimental flowchart is presented in Fig. 1(b). During the experiment, the particles were generated through a particle generator that produced KCl particles of 0.3–0.5 μm in mode value of the distribution. The qualitative and quantitative properties of the particles before and after the medium were analyzed by using a scanning mobility particle sizer (SMPS; Model 3934, TSI Inc., St. Paul, MN, USA)

Characterization of the Nanofibers

The surface morphologies of the TPFs were analyzed by using SEM (Model: 5136M). The nitrogen adsorption/desorption isotherms of the TPFs were obtained at 77 K on a Micromeritics 3H-2000PS1 volumetric adsorption analyzer. The surface voltage of the fiber was analyzed through electrometry (Model: EST103), and voltage was measured every 10 min to evaluatethe charge retention time.

RESULTS AND DISCUSSION

Characteristics of the TPFs

SEM

The surface morphologies of the electrospun PFs and TPFs examined through SEM are displayed in Fig. 2. In Fig. 2(a), the pure PFs exhibit continuous and smooth surfaces. The coarse surfaces of the TPFs are also apparent. Compared with the pure PFs, 2% TPFs were almost completely wrapped by the TiO_2 nanoparticles.

The SEM images of the TPFs supported with spunbond nylon (Fig. 3) illustrate the fiber shape of the spunbond nylon with a diameter of 20 μm. The average diameter of the TPF was approximately 240 nm, with the beads and TPF attached on the spunbond nylon as a support. The TiO_2 nanoparticles were also visible because of their agglomeration to form the rough surface of the TPFs. Compared with the pure PFs, 2% TPFs were almost completely wrapped with TiO_2 nanoparticles.

BET

The characteristics of fibers can be indentified from the adsorption/desorption isotherms by comparing with the standard classification of isotherms (Type I to Type VI) (Sing, 1985; Williams and Reed, 2006). On the other hand, the adsorption/desorption isotherms can also be explained by the typical hysteresis loop (H1–H4) (Sing, 1985). As the result shown in Fig. 4, adsorption/desorption behaviors of PFs and TPFs are closely related to the Type IV which indicate the filling and emptying of mesopores by capillary condensation ((Williams and Reed, 2006). The sharp uptake under relative pressure of 0.9–1.0 related to the existence of the voids between fibers (Jin *et al.*, 2005; Li *et al.*, 2015). In addition, typical H1 hysteresis loops can be observed in Fig. 4. Since hysteresis loop always appeared in the multilayer adsorption region, the H1 hysteresis loop also indicated the capillary condensation in uniform pores (Sing, 1985).

According to the results, the PFs and TPFs have uniform mesopores and the specific surface areas of PFs, 0.5%TPFs, 1%TPFs, 2%TPFs, and TiO_2 are listed in Table 2.These surface areas increased as TiO_2 content increased. This result was possibly due to the relatively larger surface area of TiO_2 (51.2 m^2 g^{-1}) than those of the fibers.

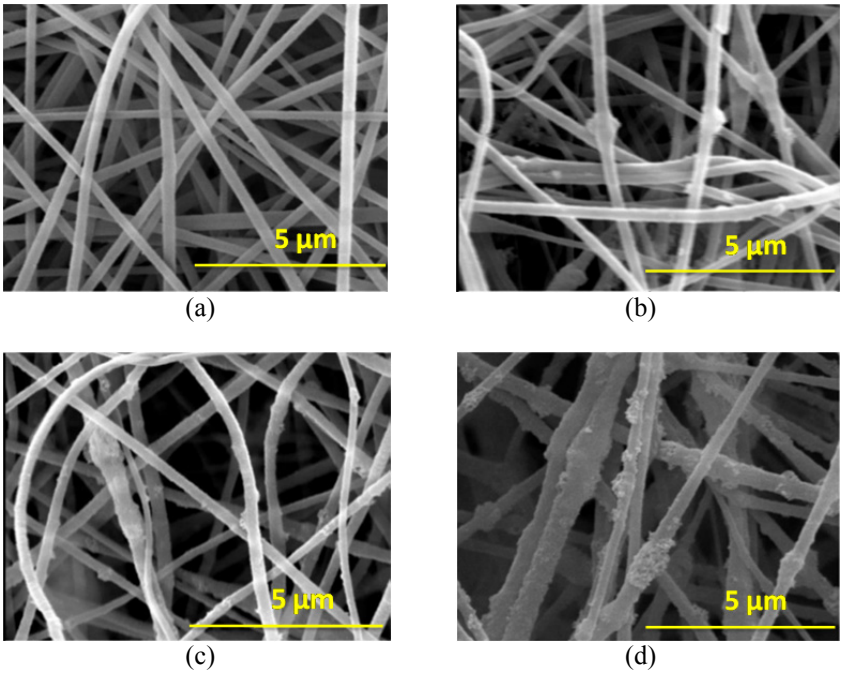

Fig. 2. SEM images of fibers with or without TiO_2 loading: (a) PFs, (b) 0.5%TPFs, (c) 1%TPFs, and (d) 2%TPFs.

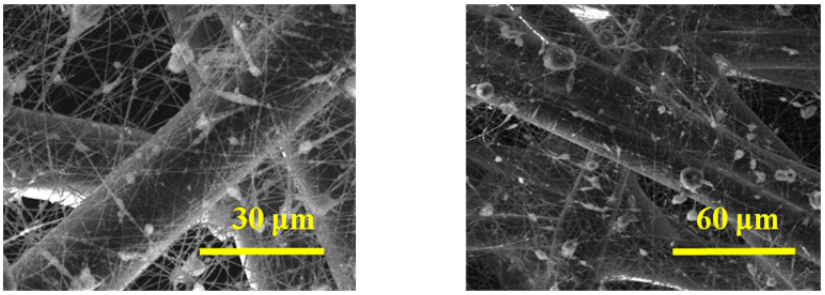

Fig. 3. SEM images of 2%TPFs.

Table 2. Surface areas of various TPFs samples.

Samples	BET Surface Area (m^2 g^{-1})
PF	3.3
0.5%TPF	6.5
1.0%TPF	8.7
2.0%TPF	13.2
TiO_2	51.2

Surface Charge Level and Temporal Decay

To understand the ability of the TPFs to maintain charge, we analyzed the surface voltage after charging through corona discharge (Table 3 and Fig. 5). A small amount of voltage was observed on the surface of the pure PF (0.74 kV). In all of the samples, the surface voltage increased with as TiO_2 loading increased. This effect could be attributed to the large and rough surface area of the materials, as confirmed through the BET method (Cho *et al.*, 2013). The smooth surface of PF facilitates the transfer of surface charge, and the large surface area of TPF is favorable for carrying charges (Lamb *et al.*, 1975; Cho *et al.*, 2013; Wan *et al.*, 2014).

Comparing the initial voltage and the voltage after 96 h, we observed that the TPFs maintained charges to a greater extent than the PFs did. This phenomenon might be attributed to the larger and rougher surface of the TPFs than that of the PFs. The surface voltage of 2% TPF decreased by 38%, which was much smaller than 57%, 50%, and 40% of the PF, 0.5%TPF, and 1%TPF, respectively. The decrease in surface charges may stabilize after this parameter decreases sharply (Igratova *et al.*, 2008). The same result was observed in our study (Fig. 5).

Particles Removal Efficiency of TFs and TPFs

Effect of Surface Voltage

The effect of surface voltage was analyzed in pure PFs and 2% TPFs with and without further charging by corona discharge. This step was included because charging can critically influence electrostatic attraction. Particle removal was efficiently achieved by the charged PFs and 2% TPFs (Fig. 6). The particle removal efficiency of the initial charged PFs and 2% TPFs was lower than that of the charged fibers. The particle penetration of TPFs was decreased from 1.89% to 0.54%, which was evidently effective than PFs (1.89% to 0.54%).This observation might be attributed to

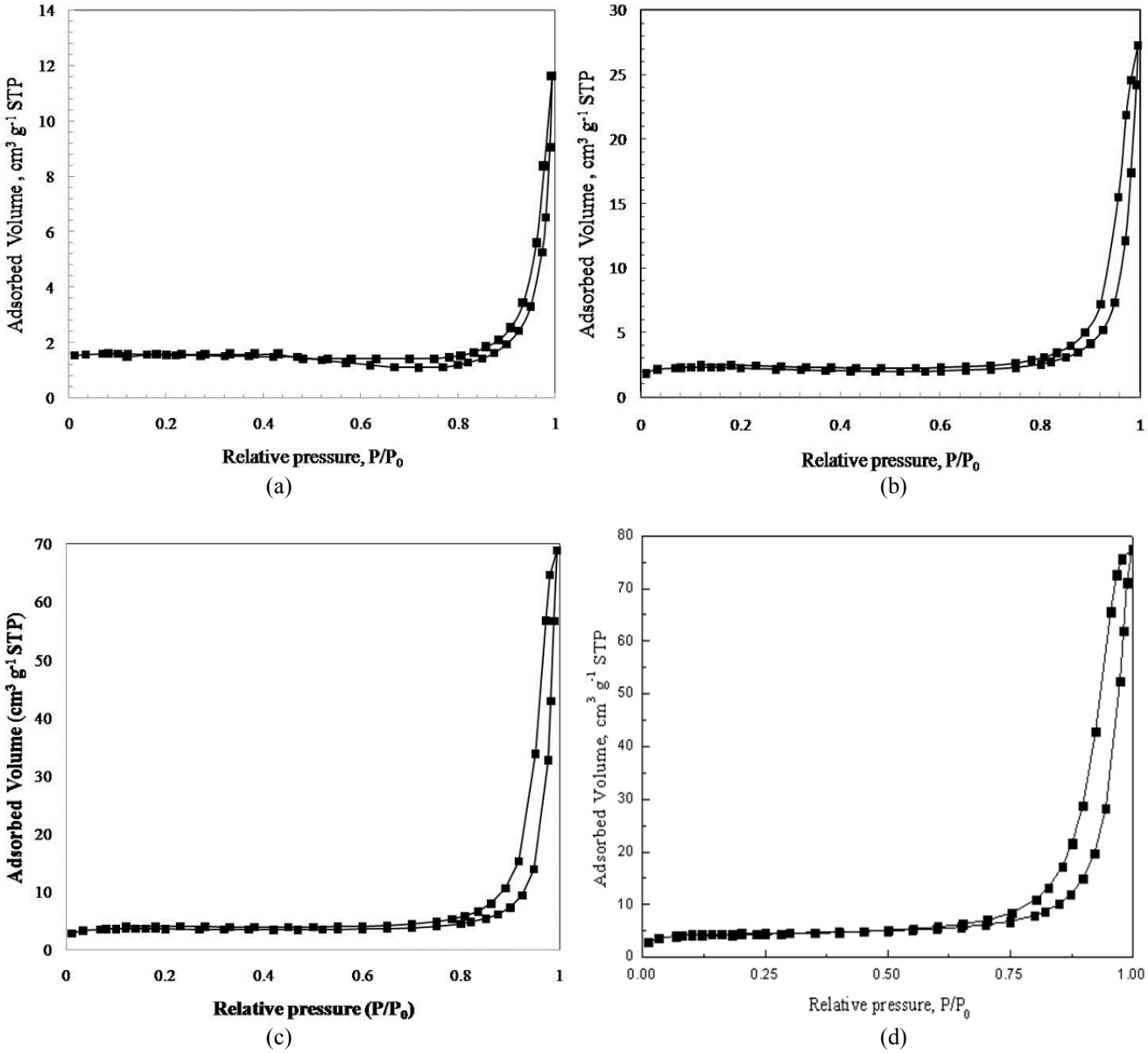

Fig. 4. N_2 adsorption-desorption isotherms of TPFs: (a) PF, (b) 0.5%TPF, (c) 1%TPF, and (d) 2%TPF.

Table 3. Surface voltage of various TPFs samples.

Samples	Initial surface voltage (kV)	Surface voltage after 96 h (kV)
PF	0.74	0.32
0.5%TPF	0.76	0.38
1.0%TPF	0.88	0.53
2.0%TPF	0.97	0.60

the TPF's larger surface area, which provided more active sites for carrying charges than those in PFs. The efficiency of particle removal can be promoted by charging the fibers or particles. This surface adsorption is affected by the surface voltage of materials.

Effect of TiO_2 Loading

Initial charged TPFs with various TiO_2 loads were analyzed using 1 g m^{-2} as weight basis at a face velocity of 0.5 cm s^{-1}. The filtration efficiency was measured for 15 min. The final particle concentrations under various particle sizes as determined by SMPS are listed in Fig. 7. Combined with the result in Fig. 6, the corona charged PF material has a higher penetration than the corona charged 2% TPF material, however the initial charged PF has a lower penetration than the initial charged 2% TPF (Fig. 7). This result may be due to the PF diameter, which was the smallest among the diameters of the test materials. This parameter may the main effluence

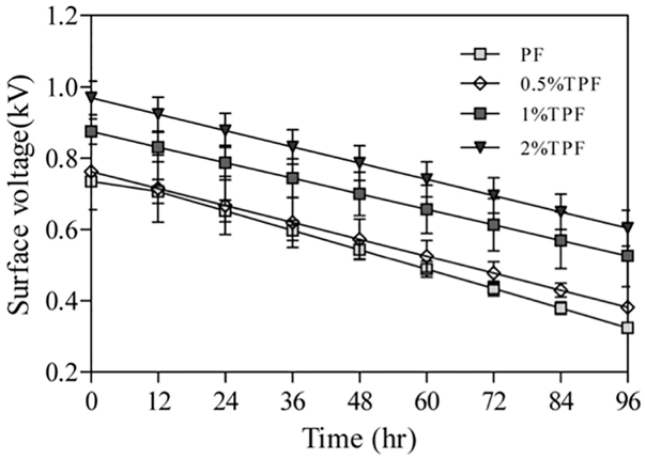

Fig. 5. Charge decay of the PFs and TPFs in every 12 hours (Temperature: 25°C; Humility: 45%).

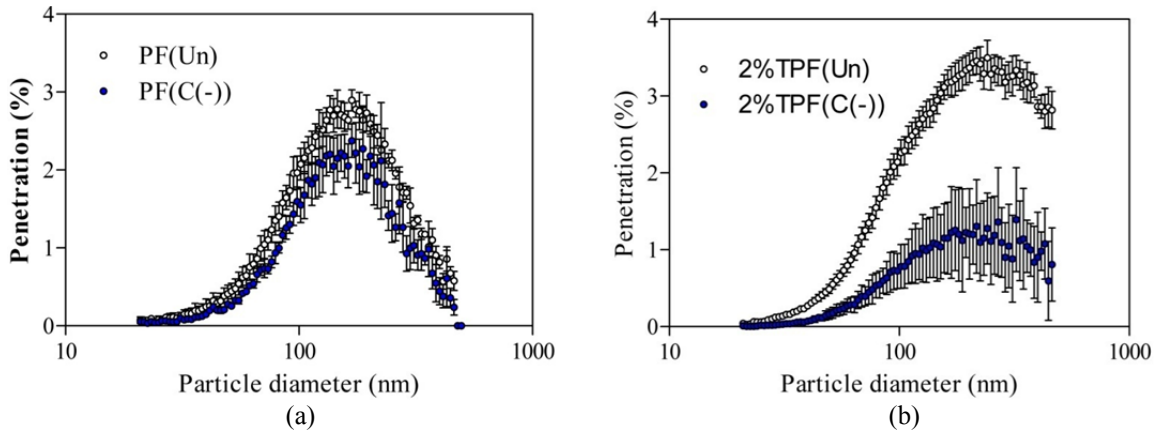

Fig. 6. Particle removal of TPFs under varies surface voltage with pure PFs and 2% TPFs ((Un) indicates the initial charged nanofibers and the (C(-)) indicates the charged nanofibers).

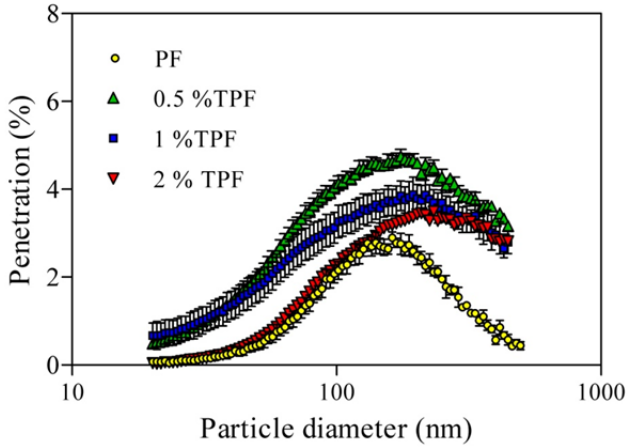

Fig. 7. Particle removal efficiency of TPFs by varies TiO_2 loading (basis weight: 1 g m^{-2}; face velocity: 0.5 cm s^{-1}).

factors for particle filtration under low surface charge (Wilcox *et al.*, 2010). In addition, the removal efficiency of initial charged TPF in this study increased as TiO_2 loading increased from 0.5% to 2%. This result is inconsistent with that of Cho *et al.* (2013), who demonstrated a considerable increase in filtration efficiency by adding TiO_2. In our research, the initial charged TPFs most efficiently removed particles at 2% TiO_2 loading, and the particle penetration (20–500 nm) was 1.83%. The increased efficiency may be attributed to the additional TiO_2 content on the TPFs, and TiO_2 potentially enhances the material surface area and provides additional active adsorption sites for particle

removal (Hung *et al.*, 2011). Surface roughness also allows the formation of an enlarged nonslip zone and expands the stagnation zone (Lamb *et al.*, 1975). The surface voltage also increased (Table 3) when the TiO_2 loading increased to improve the electrostatic attraction of particles (Fig. 6).

CONCLUSION

This study focused on the removal of particles, a major air pollutant, by TiO_2-modified nanofibers. BET and SEM results confirmed that PF and TPF charged through corona discharge significantly removed the particles because of the electrical attraction between materials with large and rough surface areas. An increase in the percentage of TiO_2 in the nanofibers correspondingly enhanced the particle removal efficiency because of the high surface charge and large surface area.

ACKNOWLEDGEMENT

This work was financially supported by Fujian province Science and Technology project Foundation (2017I01010015).

REFERENCE

Azad, A.M. and Hershey, R. (2010). Bactericidal efficacy of electrospun pure and Fe-doped titania nanofibers. *J. Mater. Res.* 25: 1761–1770.

Batool, S.S., Imran, Z., Rafiq, M.A., Hasan, M.M. and Willander, M. (2013). Investigation of dielectric relaxation behavior of electrospun titanium dioxide nanofibers using temperature dependent impedance spectroscopy. *Ceram. Int.* 39: 1775–1783.

Cai, Y., Shao, Y., and Wang, C. (2015). The Association of air pollution with the patients' visits to the department of respiratory diseases. *J. Clin. Med. Res.* 7: 551–555.

Chang D.Q., Chen S.C. and Pui D.Y.H. (2016). Capture of sub-500 nm particles using residential electret HVAC filter media-experiments and modeling. *Aerosol Air Qual. Res.* 16: 3349–3357.

Cho, D., Naydich, A. and Frey, M.W. (2013). Further improvement of air filtration efficiency of cellulose filters coated with nanofibers via inclusion of electrostatically active nanoparticles. *Polymer* 5: 2364–2372.

Choi, D.Y., Hwang, C.H., Lee, J.W., Lee, I.H., Oh, I.H. and Park, J.Y. (2013). Characterization of TiO_2 fibers prepared by combined electrospinning method and hydrothermal reaction. *Mater. Lett.* 106: 41–44.

Collins, G., Federici, J., Imura, Y. and Catalani, L.H. (2012). Charge generation, charge transport, and residual charge in the electrospinning of polymers: A review of issues and complications. *J. Appl. Phys.* 111: 044701.

Doh, S.J., Kim, C., Lee, S.G., Lee, S.J. and Kim, H. (2008). Development of photocatalytic TiO_2 nanofibers by electrospinning and its application to degradation of dye pollutants. *J. Hazard. Mater.* 154: 118–127.

Francis, L., Sreekumaran Nair, A., Jose, R., Ramakrishna, S., Thavasi, V. and Marsano, E. (2011). Fabrication and characterization of dye-sensitized solar cells from rutile nanofibers and nanorods. *Energy* 36: 627–632.

Hung, C.H. and Leung, W.W.F. (2011). Filtration of nano-aerosol using nanofiber filter under low Peclet number and transitional flow regime. *Sep. Purif. Technol.* 79: 34–42.

Ignatova, M., Yovcheva, T., Viraneva, A., Mekishev, G., Manolova, N. and Rashkov, I. (2008). Study of charge storage in the nanofibrous poly (ethylene terephthalate) electrets prepared by electrospinning or by corona discharge method. *Eur. Polym. J.* 44: 1962–1967.

Janssens, H.M., de Jongste, J.C., Hop, W.C. and Tiddens, H.A. (2003). Extra-fine particles improve lung delivery of inhaled steroids in infants: A study in an upper airway model. *Chest* 123: 2083–2088.

Jin, G., Gao, F. and Ding, X. (2005). On Classification and configuration analysis for metamorphic mechanisms. *Mech. Sci. Technol.* 7: 764–767.

Kim, H., Choi, Y., Kanuka, N., Kinoshita, H., Nishiyama, T. and Usami, T. (2009). Preparation of Pt-loaded TiO_2 nanofibers by electrospinning and their application for WGS reactions. *Appl. Catal. A* 352: 265–270.

Lamb, G.E., Costanza, P. and Miller, B. (1975). Influences of fiber geometry on the performance of nonwoven air filters. *Text. Res. J.* 45: 452–463.

Li, P., Xin, J., Wang, Y., Wang, S., Li, G., Pan, X., Liu, Z. and Wang, L. (2013). The acute effects of fine particles on respiratory mortality and morbidity in Beijing, 2004–2009. *Environ. Sci. Pollut. Res. Int.* 20: 6433–6444.

Li, Q., Satur, D.J.G., Kim, H. and Kim, H.G. (2012). Preparation of sol–gel modified electrospun TiO_2 nanofibers for improved photocatalytic decomposition of ethylene. *Mater. Lett.* 76: 169–172.

Li, X., Shi, B. and Wang, Y. (2015). Preparation of monodispersed mesoporous silica particles and their applications in adsorption of Au^{3+} and Hg^{2+} after mercapto-functionalized treatment. *Microporous Mesoporous Mater.* 214: 15–22.

Lu, H.Y., Lin, S.L., Mwangi, J.K., Wang, L.C. and Lin, H.Y. (2016). Characteristics and source apportionment of atmospheric $PM_{2.5}$ at a coastal city in southern Taiwan. *Aerosol Air Qual. Res.* 16: 1022–1034.

Nirmala, R., Kim, H.Y., Navamathavan, R., Yi, C., Won, J.J., Jeon, K., Yousef, A., Afeesh, R. and El-Newehy, M. (2012). Photocatalytic activities of electrospun tin oxide doped titanium dioxide nanofibers. *Ceram. Int.* 38: 4533–4540.

Park, S., Park, K., Yoon, H., Son, J., Min, T. and Kim, G. (2007). Apparatus for preparing electrospun nanofibers: designing an electrospinning process for nanofiber fabrication. *Polym. Int.* 56: 1361–1366.

Qiu, Y. and Yu, J. (2008). Synthesis of titanium dioxide nanotubes from electrospun fiber templates. *Solid State Commun.* 148: 556–558

Ratnesar-Shumate, S., Wu, C.Y., Wander, J., Lundgren, D., Farrah, S. and Lee, J.H. (2008). Evaluation of physical capture efficiency and disinfection capability of an iodinated biocidal filter medium. *Aerosol Air Qual. Res.* 8: 1–18

Schreuder-Gibson, H.L., Gibson, P., Tsai, P., Gupta, P. and Wilkes, G. (2005). Cooperative charging effects of fibers from electrospinning of electrically dissimilar polymers. *Int. Nonwovens J.* 13: 39–45.

Sing, K.S. (1985). Reporting physisorption data for gas/solid systems with special reference to the determination of surface area and porosity. *Pure Appl. Chem.* 57: 603–609.

Tanabe, E.H., Barros, P.M., Rodrigues, K.B. and Aguiar, M.L. (2011). Experimental investigation of deposition and removal of particles during gas filtration with various fabric filters. *Sep. Purif. Technol.* 80: 187–195.

Vega, E., Martin, M.J. and Gonzalez-Olmos, R. (2014). Integration of advanced oxidation processes at mild conditions in wet scrubbers for odourous sulphur compounds treatment. *Chemosphere* 109: 113–119.

Wan, H., Wang, N., Yang, J., Si, Y., Chen, K. and Ding, B. (2014). Hierarchically structured polysulfone/titania fibrous membranes with enhanced air filtration performance. *J. Colloid Interface Sci.* 417: 18–26.

Wang, H., Zhu, B., Shen, L., Xu, H., An, J., Pan, C. and Liu, D. (2016). Regional characteristics of air pollutants during heavy haze events in the Yangtze River Delta, China. *Aerosol Air Qual. Res.* 16: 2159–2171.

Wang, J., Mao, Y., Liu, M. and Wang, J. (2010). Numerical simulation of strongly swirling flow in cyclone separator by using an advanced RNG κ-ε model. *Acta Petrolei Sin.* 26: 8–13.

Wang, N., Yang, Y. and Al-Deyab, S.S. (2015). Ultra-light 3D nanofibre-nets binary structured nylon 6–polyacrylonitrile membranes for efficient filtration of fine particulate matter. *J. Mater. Chem. A* 3: 23946–23954.

Wen, W., Cheng, S., Liu, L., Chen, X., Wang, X., Wang, G. and Li, S. (2016). $PM_{2.5}$ chemical composition analysis in different functional subdivisions in Tangshan, China. *Aerosol Air Qual. Res.* 16: 1651–1664.

Wettervik, B., Johnson, T., Jakobsson, S., Mark, A. and Edelvik, F.A. (2015). A domain decomposition method for three species modeling of multi-electrode negative corona discharge – With applications to electrostatic precipitators. *J. Electrostat.* 77: 139–146.

Wilcox, M., Baldwin, R., Garcia-Hernandez, A. and Brun, K. (2010). Guideline for gas turbine inlet air filtration systems. *Gas Machinery Research Council*, Dallas, TX.

Williams P.T. and Reed, A.R. (2006). Development of activated carbon pore structure via physical and chemical activation of biomass fibre waste. *Biomass Bioenergy* 30: 144–152.

Zhang, S., Liu, H. and Yu, J. (2016). Microwave structured polyamide-6 nanofiber/net membrane with embedded poly (m-phenylene isophthalamide) staple fibers for effective ultrafine particle filtration. *J. Mater. Chem. A* 4: 6149–6157.

Zhang, Y., Fei, L., Jiang, X., Pan, C. and Wang, Y. (2011). Engineering nanostructured Bi_2WO_6-TiO_2 toward effective utilization of natural light in photocatalysis. *J. Am. Ceram. Soc.* 94: 4157–4161.

Zhao, M., Wang, S., Tan, J., Hua, Y., Wu, D. and Hao, J. (2016). Variation of urban atmospheric ammonia pollution and its relation with $PM_{2.5}$ chemical property in winter of Beijing, China. *Aerosol Air Qual. Res.* 16: 1378–1389.

Zhu, Z., Ji, Y., Zhang, S., Zhao, J. and Zhao, J. (2016). Phthalate ester concentrations, sources, and risks in the ambient air of Tianjin, China. *Aerosol Air Qual. Res.* 16: 2294–2301.

Received for review, July 15, 2016
Revised, May 14, 2017
Accepted, June 6, 2017